

ADVANCING CONDITION ASSESSMENT OF REINFORCED CONCRETE BRIDGE ELEMENTS THROUGH AUTOMATION, VISUALIZATION, AND IMPROVED INTERPRETATION OF MULTI-NDE TECHNOLOGY DATA

ВДОСКОНАЛЕННЯ ОЦІНКИ СТАНУ ЗАЛІЗОБЕТОННИХ ЕЛЕМЕНТІВ МОСТІВ ШЛЯХОМ АВТОМАТИЗАЦІЇ, ВІЗУАЛІЗАЦІЇ ТА ПОКРАЩЕННЯ ІНТЕРПРЕТАЦІЇ ДАНИХ ЗА ДОПОМОГОЮ КОМПЛЕКСНОЇ ТЕХНОЛОГІЇ ОБСТЕЖЕННЯ НЕРУЙНІВНИМИ МЕТОДАМИ

Nenad Gucunski*, Hung Manh La†, Kien Dinh‡, and Mustafa Khudhair§

*Rutgers University, Department of Civil and Environmental Engineering; gucunski@soe.rutgers.edu

†University of Nevada-Reno, Department of Computer Science and Engineering

‡NDT Concrete LLC

§Rutgers University, Department of Civil and Environmental Engineering

Economic bridge management requires accurate information about the condition of bridges in the network. Nondestructive evaluation (NDE) has shown high potential in providing accurate condition assessment and, through periodic surveys, development of accurate deterioration, predictive, and life-cycle cost models. To achieve wide adoption by transportation agencies, further advances should be made that would lead to the accuracy of NDE-based condition assessment, reduced costs and traffic interruptions, and minimized risk to transportation workers. The paper discusses the following areas of improvement: increased speed and safety of data collection through the use of robotic systems, and improved data interpretation through visualization and joint analysis of data collected by multiple NDE technologies.

Ефективне з економічної точки зору управління процесом експлуатації мостів вимагає точної інформації про їх стан. Обстеження неруйнівними методами (NDE) продемонструвало високий потенціал у забезпеченні точності оцінки технічного стану та прогнозування фінансових витрат протягом життєвого циклу завдяки розробці точних моделей деградації, створених на базі результатів періодичних обстежень. Для широкого впровадження цих методів транспортними агентствами слід досягти подальших успіхів, які призведуть до підвищення точності оцінок технічного стану на основі NDE, зменшать витрати та перебої в русі, а також зведуть до мінімуму ризик для працівників транспорту. У статті обговорюються наступні напрямки вдосконалення: підвищення швидкості та безпеки збору даних завдяки використанню роботизованих систем, а також покращення інтерпретації даних шляхом візуалізації та спільного аналізу даних, зібраних із використанням кількох технологій NDE.

Keywords: reinforced concrete, bridges, GPR, impact echo, ultrasonic surface waves, ultrasonic tomography, electrical resistivity, half-cell potential, visualization

Ключові слова: залізобетон, мости, георадар, ударний ехо-метод, ультразвукові поверхневі хвилі, ультразвукова томографія, електричний опір, гальванічний потенціал, візуалізація

Introduction

Deterioration in reinforced concrete (RC) bridge components is a result of a multitude of actions. Some of the physical factors include repeated application of heavy traffic loading, thermal effects, shrinkage, and freeze-thaw cycles. However, and more often, chemical factors like reinforcement corrosion, alkali-silica reaction, or carbonation have a dominant influence on the deterioration processes. As a result of all these described actions, multiple deterioration and defects will be generated in bridge elements. According to the ASCE 2021 Infrastructure Report (ASCE 2021), nearly 231 000 bridges in the United States need repair and preservation work, and about 5.5% of the bridge deck area is designated as structurally deficient or poor. To improve bridge conditions in the next dec-

ade, it is estimated that an increase in annual spending on bridge rehabilitation from US\$14.4B to US\$22.7B will be needed. Improving the accuracy in the detection and characterization of deterioration and defects of reinforced concrete bridge elements using nondestructive evaluation (NDE) methods is essential for an accurate assessment of best rehabilitation and repair procedures. The condition assessment, paired with an improved speed of NDE data collection and interpretation, will allow economical periodical evaluation of bridges. Such periodical assessments will enable the capture of deterioration processes and defect formation, leading to the development of more accurate deterioration, predictive, and life-cycle cost models (Gucunski et al. 2016; Kim et al. 2019). Ultimately, these will lead to better bridge management.

This paper provides an overview of the current practice of bridge evaluation by NDE methods, recent efforts to improve the speed of NDE data collection through automation and robotics, and improved condition interpretation through advanced visualization and combined analysis of results of multiple NDE technologies. Automation of NDE data collection for bridges in the past 10 years concentrated on the assessment of bridge decks, because they deteriorate faster than other bridge components and the deployment of NDE technologies is simpler. Several automated and robotic systems deploying single or multiple NDE technologies have been developed. Most of the systems enable data collection with high spatial resolution through the use of large sensor arrays or multiple probes. On the other hand, the development of robotic systems for other bridge elements with vertical surfaces is far more challenging. Climbing robots for vertical elements have been designed and developed with different locomotion and adhesion methods.

The characteristics, challenges, and applications of these systems are presented. On the condition interpretation side, the results of NDE surveys of bridge elements are most commonly presented in terms of condition maps based on the data collected by particular NDE technologies. While those are essential to describe the surface projection of the location and the severity of deterioration and defects, both elements can be improved through 3D data visualization and joint analysis of data from multiple NDE technologies. The paper specifically discusses recent developments in 3D visualization of ground penetrating radar (GPR) and ultrasonic shear wave data for concrete structures. The combination of these two technologies enables the mapping of reinforce-

ment and clear visualization of the most common defects in concrete such as delamination, rebar debonding, corrosion, honeycombing, and such. Finally, while the use of multiple NDE technologies enables comprehensive evaluation, each NDE technology has limitations due to different parameters affecting the measured values and, thus, the interpretation of their results. To improve the interpretation, a joint analysis of data collected by multiple NDE techniques using machine-learning algorithms that incorporate various influencing parameters or other approaches can be implemented. These are discussed and examples are presented.

Current Practice of Condition Assessment of RC Bridges by Manual NDE Technologies

Deterioration processes in bridge components are often complex and are, thus, manifested through multiple deterioration indicators which can be detected and characterized by different NDE technologies. Some of the technologies can detect and evaluate only a single deterioration indicator, while some can evaluate multiple ones. In addition to defect and deterioration detectability, the methods significantly differ in the speed of data collection and interpretation, ease of use, cost, and level of expertise needed in both data collection and analysis. The following sections describe condition assessment by manual NDE technologies on concrete bridge decks and other superstructure and substructure RC components.

Condition assessment of concrete bridge decks by NDE most commonly concentrates on the evaluation of the state of corrosion, delamination, and concrete quality. It is commonly done on a test grid, for example, 60 × 60 cm (2 × 2 ft), as shown in Figure 1. A comprehensive condition assessment re-



Figure 1. Manual NDE data collection on a bridge deck (a) using the following NDE technologies: (b) impact echo; (IE); (c) ground penetrating radar (GPR); (d) ultrasonic surface waves (USW) and electrical resistivity (ER); (e) half-cell potential (HCP)
 Рис. 1. Ручний збір даних NDE на настилі мосту (а) з використанням наступних технологій NDE: (б) ударний ехо-метод (ІЕ); (с) георадар (GPR); (д) ультразвукові поверхневі хвилі (USW) і вимірювання електричного опору (ER); (е) гальванічного потенціалу (HCP)

quires the use of multiple technologies. As shown in the figure, five NDE technologies are simultaneously deployed to evaluate the three states. The corrosion evaluation primarily relies on the electrical resistivity (ER) and half-cell potential (HCP) methods, and GPR as a secondary method. The delamination assessment primarily relies on the impact echo (IE) method, with ultrasonic surface waves (USW) and GPR as secondary methods. Finally, USW is a method that provides a quantitative assessment of concrete quality, while GPR is considered a qualitative tool. The results of evaluations are typically presented in terms of condition maps, as shown in the following section in Figure 4.

ER evaluates the corrosive environment of concrete by measuring the resistivity of concrete, which is significantly influenced by the moisture content (Nguyen et al. 2017), chloride concentration (Rupnow and Icenogle 2012), and the presence of cracks. The resistance can be related to the normally observed corrosion rates (Gowers and Millard 1999; Hornbostel et al. 2013). The most commonly used probe for field evaluation is a four-point Wenner probe, shown in Figure 1, which conforms with AASHTO TP 95-11 specifications. On the other hand, HCP provides information about the probability of active corrosion of reinforcement (ASTM C876-15). The method can be used at any time during the life of a concrete structure provided the temperature is above 20C (Elsener et al. 2003). HCP has a maximum penetration depth of around 200 mm (Bien et al. 2007). There are different types of HCP probes, also called reference electrodes. A rolling HCP probe is shown in Figures 1 and 2. Because the probe needs to be connected to the steel reinforcement, and the reinforcement needs to be connected to provide continuity throughout the survey area, the method is not

appropriate for inclusion in automated or robotic systems.

Delamination detection and characterization are primarily done using acoustic methods. Among acoustic methods, impact echo is the most commonly used. IE examines the transient response of a plate-like structure subjected to an acoustic pulse. The objective of the IE test is to detect resonant modes (Sansalone and Carino 1989). The peaks in the response spectrum represent either the thickness stretch Lamb wave modes (Gibson and Popovics 2005) or flexural modes (Kee and Gucunski 2016). The delamination depth can be obtained from the resonant frequency. In the case of shallow delamination (shallower than about 50 mm), where the resonant frequency is high, a more reliable approach is using a constant-phase IE approach (Almallah and Gucunski 2019). Air-coupled IE, in which contact sensors are replaced by microphones (Zhu and Popovics 2007) or MEMS (Sun et al. 2018), opens opportunities for rapid data collection. Another acoustic method that will be discussed later, ultrasonic tomography (UST), provides more detailed imaging of delaminated elements. Finally, shallow delamination can be rapidly detected using infrared thermography (IRT) (Maser and Roddis 1990; Maierhofer et al. 2001). However, delamination detection significantly depends on environmental conditions (Washer et al. 2009).

The quantitative assessment of concrete quality is most frequently assessed by the measurement of concrete elastic modulus using the USW method (Nazarian et al. 1994). The USW modulus evaluation relies on the measurement of the velocity of propagation of surface waves of wavelengths shorter than the deck thickness. The presence of shallow delamination often leads to the measurement of an apparent low concrete modulus (Azari et al. 2012). Typical USW devices

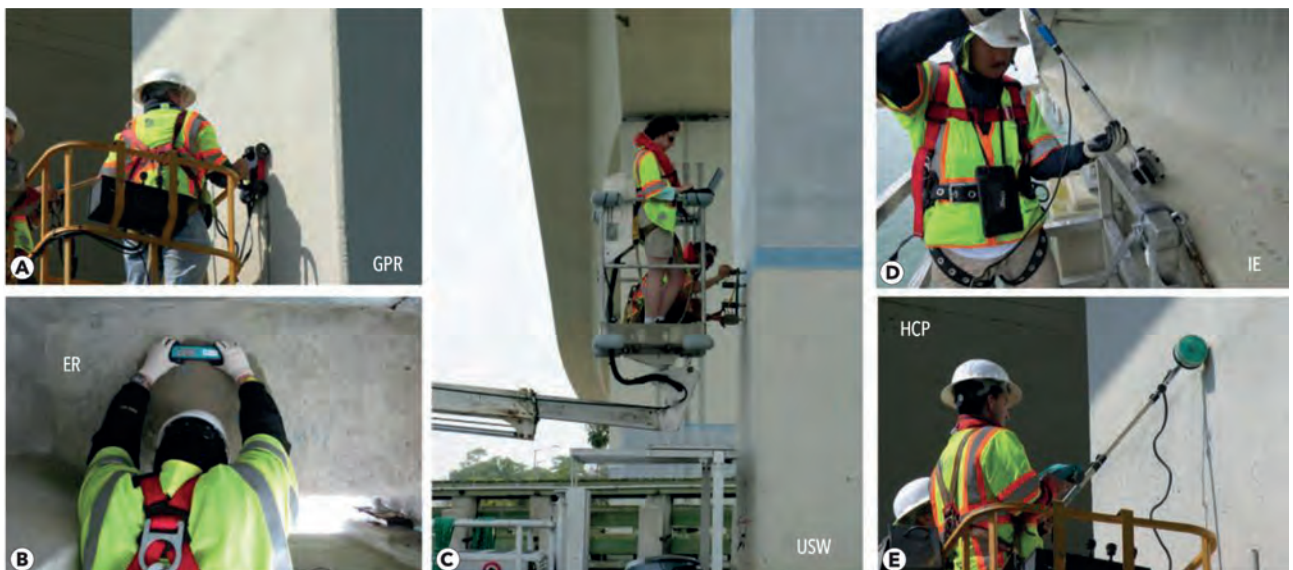


Figure 2. Manual NDE data collection on bridge piers and girders: (a) GPR; (b) ER; (c) USW; (d) IE; (e) HCP

Рис. 2. Ручний збір даних NDE про опори та балки мостів: (а) георадар; (б) ER; (с) USW; (д) IE; (е) HCP

consist of a source and two receivers. One of the devices, the portable seismic property analyzer (PSPA), is shown in Figures 1 and 2. GPR provides a qualitative assessment of the deck condition. The condition assessment is based on the evaluation of the amplitude of electromagnetic waves reflected from the top rebar layer (Barnes and Trottier 2000; Maser and Bernhardt 2000; Tarussov et al. 2013). Using certain thresholds, most often related to the results from other NDE technologies, areas with high signal attenuation in the obtained map are described as deteriorated concrete (Barnes et al. 2008). Consideration of the variability of concrete cover thickness and concrete conductivity is essential for an accurate assessment of signal attenuation (Dinh et al. 2016). Bridge deck evaluation by GPR can be conducted using ground-coupled (Figure 1) and air-coupled antennas. Typical productivity for ER, HCP, and IE data collection using the shown devices is about 100 m² (1000 ft²) on a 60 × 60 cm (2 × 2 ft) test grid. It is about 25 m² (250 ft²) for USW and about 500 m² (5000 ft²) for GPR on survey lines with a 60 cm (2 ft) spacing. More information about the performance of NDE technologies for the condition assessment of bridge decks can be found in an SHRP 2 report (Gucunski et al. 2013).

Condition assessment of other bridge components can be done using the same NDE technologies and devices as for concrete bridge decks. The biggest challenge in the NDE technology deployment is access to the element to be evaluated. The application of the previously described five NDE technologies in the condition assessment of concrete bridge piers and prestressed girders is shown in Figure 2.

Automation of NDE Data Collection

Comprehensive condition assessment of concrete bridges can be done using manual NDE technologies. However, and as illustrated in the previous section, manual multi-NDE technology data collection requires significant time and effort. In addition, in bridge deck evaluation, and in cases when super-

structure and substructure evaluation is done using snoopers, work zones for inspection cause traffic interruptions. All are adding to the cost of inspections, slowing or interrupting the traffic flow, and increasing risks for the inspectors and the traveling public. Considering that there are more than 620 000 bridges in the US, manual inspection and condition monitoring of the bridge network using NDE is not feasible. Automation of NDE data collection is, therefore, critical for their wide adoption as a tool for accurate condition assessment and monitoring and, thus, economic bridge management. The following sections describe some efforts in the automation of NDE data collection in the inspection of bridge decks and other bridge components.

Automation of Bridge Deck NDE

One of the earliest attempts for automated multi-NDE of concrete bridge decks was the robotic system BETOSCAN developed at the German Federal Institute for Material Research and Testing (BAM) (Raupach et al. 2009). BETOSCAN enabled the deployment of multiple NDE devices: ultrasonic, potential mapping, microwaves, and cover meters. While the system had significant capabilities, it could be deployed in the evaluation of smaller areas only because of a single NDE sensor installation. The RABIT (Robotics Assisted Bridge Inspection Tool) platform (Gucunski et al. 2017) brings elements of the previous efforts and implements them in a much bigger robotic platform with multiple NDE devices or sensor arrays (Figure 3).

RABIT integrates four NDE technologies: ER, GPR, USW, and IE. There are four ER probes and two acoustic arrays on the front end of the platform. The two acoustic arrays are equivalent to 16 IE devices and 12 USW devices. Two GPR arrays are mounted on the rear end of the platform, each having eight antenna pairs of dual polarization. Finally, two high-resolution cameras for deck surface imaging are mounted on the front end. RABIT is a fully autonomous system, whose

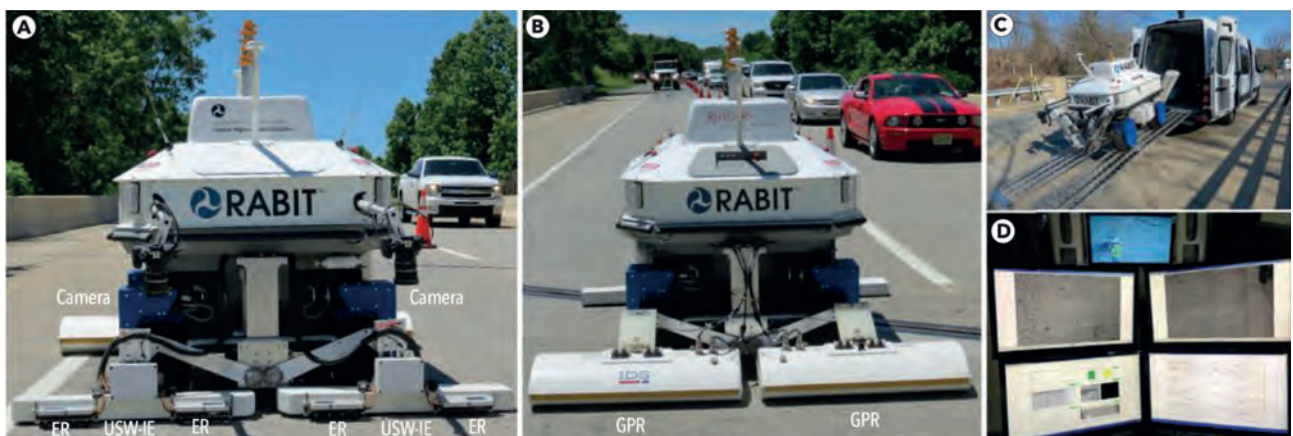


Figure 3. Robotic platform RABIT: (a) front view; (b) back view; (c) unloading from the command van; (d) screens in the command van. Рис. 3. Роботизована платформа RABIT: (а) вид спереду; (б) вид ззаду; (с) розвантаження з машини управління; (д) монітори в машині управління

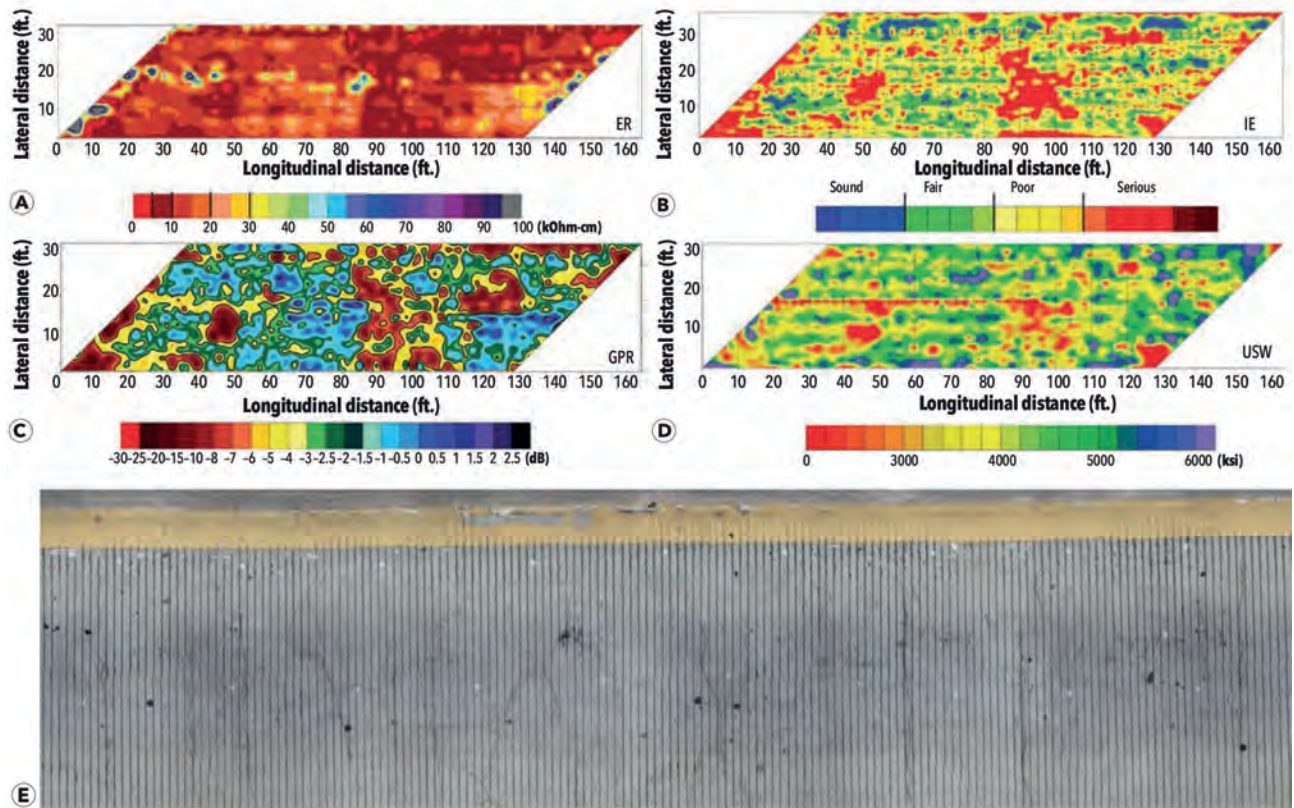


Figure 4. Condition maps from four NDE technology surveys: (a) ER; (b) IE; (c) GPR; (d) USW; and (e) section of the deck surface image
 Рис. 4. Карти стану бетону за результатами чотирьох технологічних досліджень NDE: (а) ER; (b) IE; (с) георадар; (d) USW; та (е) зображення фрагменту поверхні настилу мосту

navigation was achieved through an integration of the differential global positioning system (DGPS), inertial measurement unit (IMU), and the wheel odometry. The data collection path is preprogrammed in terms of the deck sections to be evaluated and increments in the data collection. All the NDE data are streamed and monitored in real-time in the command van (Figure 3). The data collection production rate depends on the length of the bridge and data collection increment. For bridge decks approximately 100 m (330 ft) long, and data collection increment of 0.6 m (2 ft), RABIT can evaluate about 350 to 400 m² (3500 to 4000 ft²) per hour.

A sample of results from the RABIT includes the condition maps of a bridge shown in Figure 4, the ER map describing the severity of the corrosive environment, the IE delamination map, and GPR and USW maps of qualitative and quantitative concrete quality assessment. The condition maps are complemented by a high-resolution image of the deck surface which is obtained from stitched camera images. A section of the bridge deck with visible cracks is shown in the same figure. Such images become permanent records of the deck surface that can be reviewed at any time.

While the data collection speed of RABIT is significantly higher than of the manual data collection (approximately three times higher than a team of five NDE technicians), it could be significantly increased

through the use of air-coupled and/or rolling probes that would eliminate RABIT's test point stops. As an example, the use of air-coupled acoustic and vertical electrical impedance (alternative to ER) testing, along with GPR and high-definition imaging, was implemented on an NDE platform that enabled data collection at a walking speed (Pashtouni et al. 2020).

Climbing Robots for Bridge Superstructure and Substructure

The development of climbing robot systems for bridge inspection has received great attention recently (Tirthankar et al. 2018; Nguyen and La 2021). Inspired by the way that animals and insects move, robots have demonstrated the feasibility of climbing over different connectors and surfaces on bridges (Minor et al. 2000; Nguyen and La 2019; Nguyen et al. 2020). However, each bridge has many locations to be checked, and they are usually not close together, so it will take a long time for those climbing robots to complete the inspection of a bridge, not to mention that the calculation to move also takes a lot of time and requires intelligent algorithms. Studies on using drones for inspection have found that drones allow a quick, efficient overview without being limited to the bridge element material. However, a comprehensive inspection of bridges requires multiple positions for in-depth testing, while the current drone capabilities can provide only a visual inspection. Unlike the approaches mentioned

above, a new hybrid robotic design is presented, which considers the advantages of a drone's flying flexibility and a mobile robot's steady climbing capability to perform in-depth inspections of bridges. With the new design, the in-depth inspection of the bridge will also be conducted faster because of the drone's maneuverability. The mobile robot part is equipped with permanent magnets that can change the distance from the steel surface. Changing the distance between the magnet and the steel surface allows the robot to switch its operating modes between landing, taking off, and moving.

The design concept of this robot is illustrated in Figure 5. The robot is integrated with multiple sensors: Intel camera T265 and GPS for robot location tracking, infrared sensors for a safe landing, and a GMR sensor for crack detection. The onboard computer for processing is a Raspberry Pi4. The PX4 flight controller is for controlling the robot. The robot is surrounded by a sphere cage to protect it from a collision with the bridge. Overall, the robot is designed to work in two modes: mobile and drone. The mobile part allows the robot to cling to steel surfaces and move like other conventional mobile robots.

A new robot version will be able to cling to any material type surface, including concrete. On the robot, the body is attached to magnets to create an attractive force when the robot clings to a steel surface. The distance between the magnet array and the steel face is controlled by two pull motors. This distance is adjusted depending on the working condition of the robot. If the robot needs to cling strongly to the structure, then the distance is 0. Several images of the robot climbing on vertical structures of the bridge are shown in Figure 5. The robot was in mobile mode, using its wheels to climb on the elements. As shown, the robot can climb on tall elements and access difficult-to-reach areas to perform inspections. If the robot needs to climb on the bridge, then the distance is larger than 0 (e.g., 0.3 cm) to allow easy crawling of the robot. The drone mode allows the robot to fly between inspection areas. In this mode, the robot uses a high-resolution camera to capture images or record video of the surface of the bridge elements and joints. At the same time, the robot sends images to the inspector for live viewing. To navigate the robot in the drone mode, the inspector wears a VR headset (5.8 GHz) to receive video data from the ro-

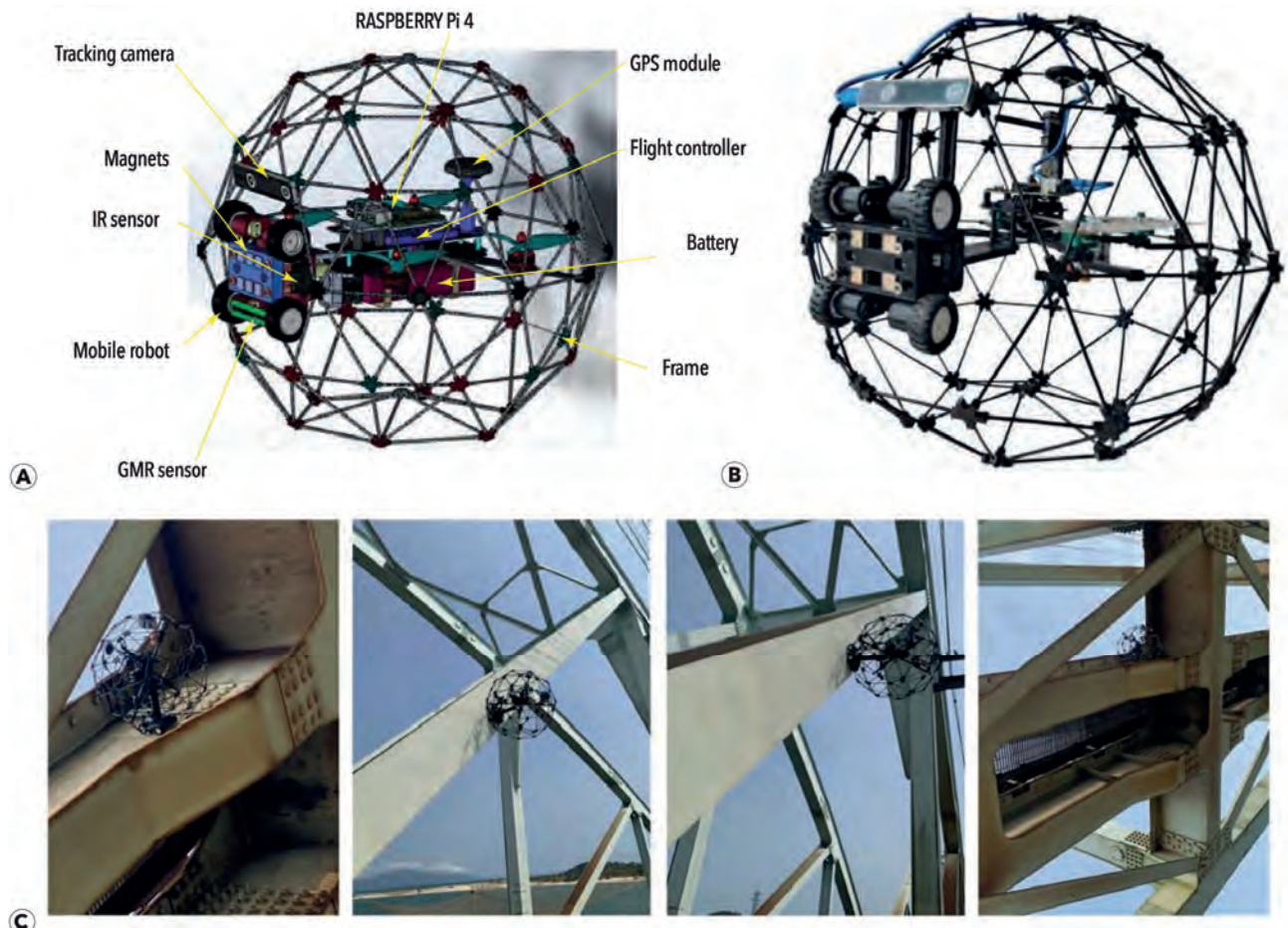


Figure 5. Flying robot with sensor integration: (a) overall design; (b) as built; and (c) images of the robot climbing on vertical surfaces of steel bridge elements

Рис. 5. Літаючий робот із вбудованими датчиками: (а) загальна будова; (б) в зборі; та (с) зображення робота, що піднімається на вертикальні поверхні сталевих елементів мосту



Figure 6. A snapshot from a recorded video taken by the robot. Two zoomed-in areas on the right side show the crack location
 Рис. 6. Знімок із записаного відео, який зроблено роботом. Дві збільшені області праворуч показують розташування тріщини

bot's camera for observation of the environment at a distance of up to around 2 km. The robot uses its camera to detect available surfaces to land on the element (switching from the flying to the mobile mode). The robot relies on the values of two infrared sensors along with an intelligent landing algorithm to determine if the point in front is a safe position to land.

The robot was deployed to collect data on several bridges. Both mobile and drone modes were tested to validate the design. The left side of Figure 6 shows a snapshot of a video recording of a highway bridge taken by the robot in the flying mode. There are two high-resolution images on the right of the figure showing cracked pier surface areas from the robot's flight close to the pier.

Advanced Data Visualization

Like the automation discussed above, 3D visualization of NDE data is another area where improvements can be made for a more comprehensive and effective assessment of concrete bridges. Visualization allows NDE data to be presented in an intuitive manner, which will, in turn, facilitate the understanding and further analysis of NDE test results. Unlike the conventional data processing methods, which are used to detect the presence of anomalies through measurement of different physical properties of concrete, data visualization may help identify the exact location and shape of structural defects. As an example, it is known that the data collected by GPR contain significant information about the bridge deck condition (Tarussov et al. 2013). However, a major drawback of it is that its data in raw form are complex in nature, large in volume, and difficult to understand, and therefore can only be analyzed by GPR experts (Gucunski et al. 2013; Tarussov et al. 2013; Dinh et al. 2019). Even when GPR data are interpreted by GPR experts, the process is usually time-con-

suming and labor-intensive. In addition, the results can vary significantly between analysts. As illustrated in the subsequent paragraphs, these issues can be minimized, if not eliminated, through developing a standard procedure for visualizing and analyzing 3D images. It is noted that, while 3D visualization can be implemented for various technologies (Kim et al. 2017), herein it is demonstrated in the data collected by GPR and ultrasonic shear wave imaging devices.

GPR was developed originally as a geophysical imaging technique (Daniels 2004). GPR experts would review the collected GPR data, usually in the form of B-scans, to identify different subsurface layers and/or anomalies. For concrete applications, the evaluation results are conventionally presented in the form of contour maps of rebar reflection amplitude, on which the areas of low signal amplitude indicate the likelihood of rebar corrosion and/or concrete delamination, as was shown in Figure 4. Although this method has been validated for many bridge decks, it also has some significant limitations, as pointed out in the existing literature. First, the method can lead to deceptive results due to factors affecting the amplitudes such as depth, surface anomalies, reinforcing bar spacing, reinforcing bar configuration, and polarization effects (Tarussov et al. 2013). Second, it is not suitable for analyzing time-series data with the possibility of suggesting false improvement of the concrete condition over time (Dinh et al. 2015). The ability to map the locations of rebars, tendons, voids, concrete delaminations, and so on, is of great interest to fully understand the condition of concrete bridge elements. The benefit of 3D visualization for the condition assessment of concrete bridges is illustrated in Figure 7. In this figure, the conventional method for presenting the condition map (Figure 7a) is compared with the one based on the 3D visualization technique (Figure 7b) for a concrete deck where a significant amount of salt was added to concrete mixes during construction in one section of the deck. The resulting areas of a highly corrosive environment are marked on the maps. With such ground-truth information, one can easily observe in Figure 7a, the areas of false-positive diagnosis of a highly corrosive environment associated with the conventional method. As a comparison, that is not the case with the map in Figure 7b, which clearly shows the locations of all rebars as well as the sections of rebars affected by corrosion.

Ultrasonic shear wave tomography has recently become a commonly used technology for imaging concrete structures. It works by using multiple dry-point-contact (DPC) transducers to transmit and receive shear wave signals (De La Haza et al. 2013). The data obtained from a large number of transducer couples/pairs are then used to reconstruct the interior/volumetric image of concrete. A 3D image created from such data for a section of

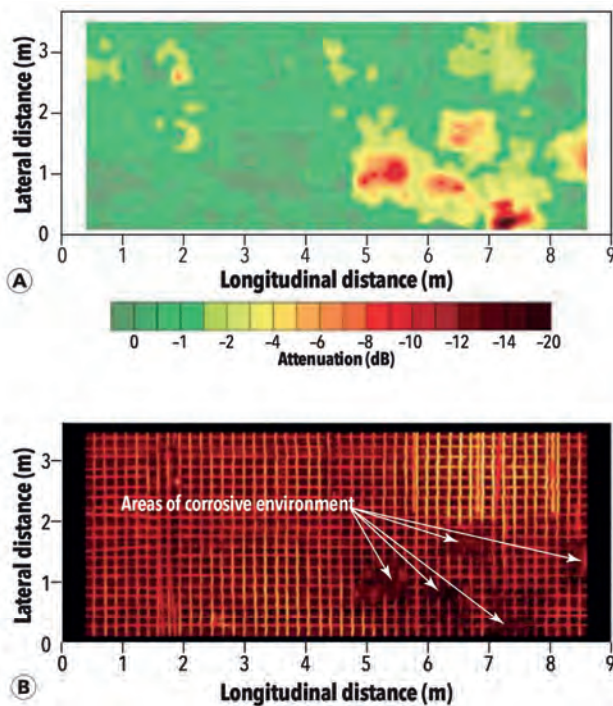


Figure 7. Presenting concrete bridge deck condition: (a) conventional method; (b) 3D visualization method (Dinh et al. 2019)

Рис. 7. Відображення стану бетонного мостового покриття: (a) звичайний метод; (b) метод 3D-візуалізації (Dinh et al. 2019)

the above concrete bridge deck specimen is shown in Figure 8. The image clearly shows the locations and shapes of simulated delamination, which was embedded into the deck during construction. It is worth noting that a delaminated area caused by corrosion is displayed in the image. This area coincides with an area of the corrosive environment depicted in Figure 7. The delamination is visible in the 3D image created from the ultrasonic shear wave data. The same is not the case with the one reconstructed from the GPR data. According to Dinh and Gucunski (2021), some factors might affect the visibility of delamination in GPR images such as the thickness of delamination, antenna frequency, signal attenuation, the proximity of steel bars, and so on. On one side, this indicates the need for using multiple NDE technologies for a comprehensive evaluation of concrete bridge elements. On the other side, which is of more interest to this section, it

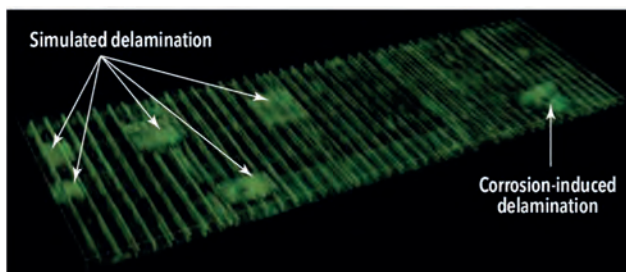


Figure 8. 3D visualization of bridge deck specimen from ultrasonic shear wave data

Рис. 8. 3D-візуалізація зразка мостового покриття за даними ультразвукової зсувної хвилі

showcases the benefits of 3D visualization of NDE data for concrete bridges.

Improved Interpretation of Multi-NDE Technology Data

It has been recognized that NDE results may be affected by many parameters such as the degree of saturation, concrete cover, delamination depth, and similar. For example, Robles et al. (2022) summarized the effects of multiple parameters, including temperature, the presence of steel reinforcement, cracks and delamination defects, specimen geometry, and concrete composition on ER results. Because of that, corrections including the effects of those parameters should be incorporated to improve the data interpretation, which can be achieved through a joint analysis of results from multiple NDE technologies.

The joint analysis approach is illustrated for the HCP data collected on a bridge specimen at the BEAST (Bridge Evaluation and Accelerated Structural Testing) facility at Rutgers University. The measured potential of corrosion activity is, among others, affected by the moisture content of concrete, concrete cover thickness, presence and moisture condition of delamination, and electrical resistivity of concrete. The four parameters can be evaluated using different NDE technologies, as illustrated in Figure 9. For example, the Moist-SCAN device (Goeller and Jungstadt 2018) was used to estimate the degree of saturation of the concrete slab, as shown in Figure 9a. On the other hand, the concrete cover thickness was obtained from the GPR survey, as shown in Figure 9b. The IE results provide information about the delamination location and depth, as shown in Figure 9c. In addition, the results of ER measurements, as shown in Figure 9d, have been taken into consideration to correct the HCP measurement results.

To enable improved data interpretation, a series of finite element models have been prepared to simulate the effect of mentioned parameters on the results of various NDE technologies using COMSOL Multiphysics software. The results of the finite element models were used to produce an algorithm that mitigates the effects of different parameters on the results of the HCP. The effect of two of the parameters—the moisture content and concrete cover thickness—is illustrated in Figure 10. The HCP results before and after applying the algorithm are shown in the same figure. The raw HCP data in Figure 10c shows that the middle area of the slab has high potential values (more negative values) indicating an anticipated high corrosion activity, while the edges tend to have fewer negative values. On the other hand, the HCP measurement is modified based on four different parameters: the degree of saturation, concrete cover, delamination depth, and electrical resistivity, which are shown in Figure 10d. It can be seen clearly that the algorithm

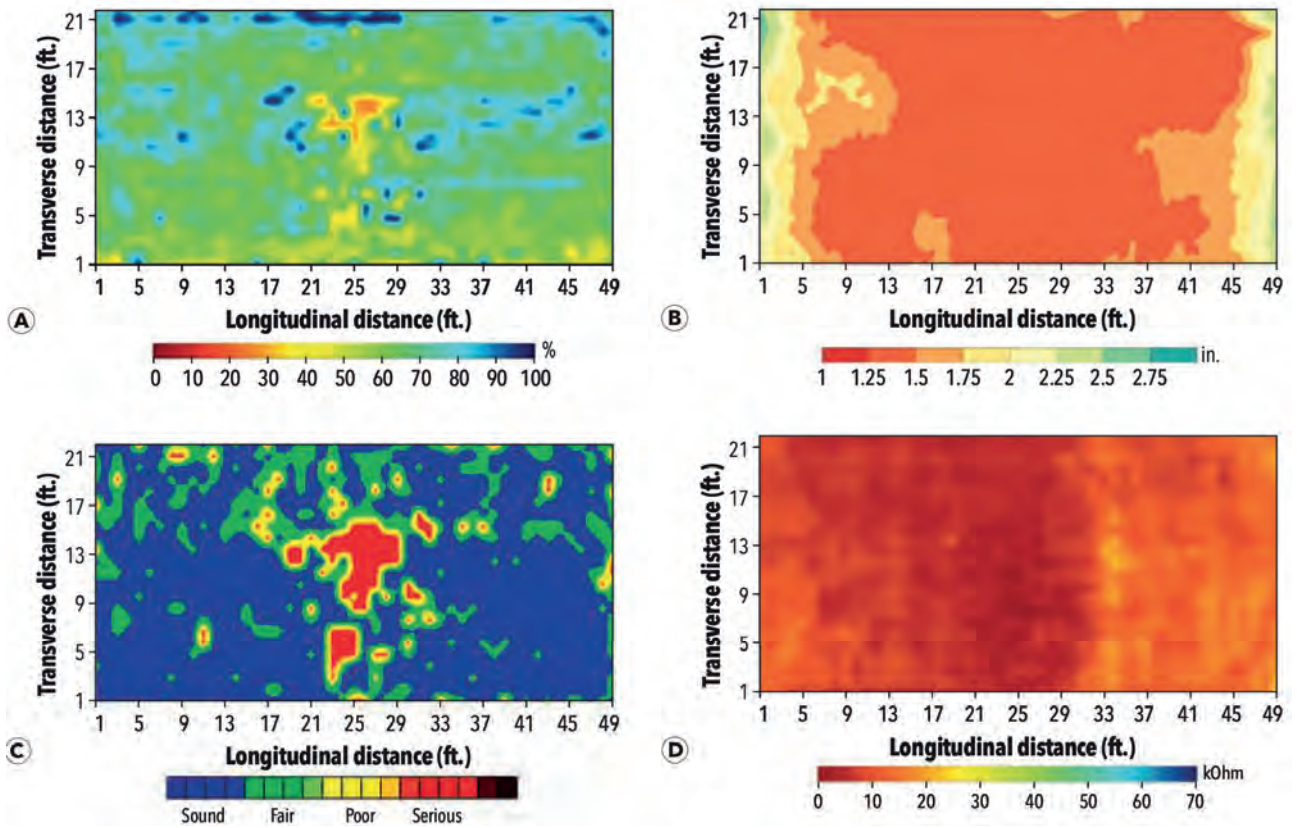


Figure 9. NDE maps for the BEAST slab: (a) degree of saturation; (b) concrete cover; (c) delamination; (d) electrical resistivity
 Рис. 9. Карти NDE для плити BEAST: (a) ступінь насичення; (b) бетонне покриття; (c) розшарування; (d) електричний опір

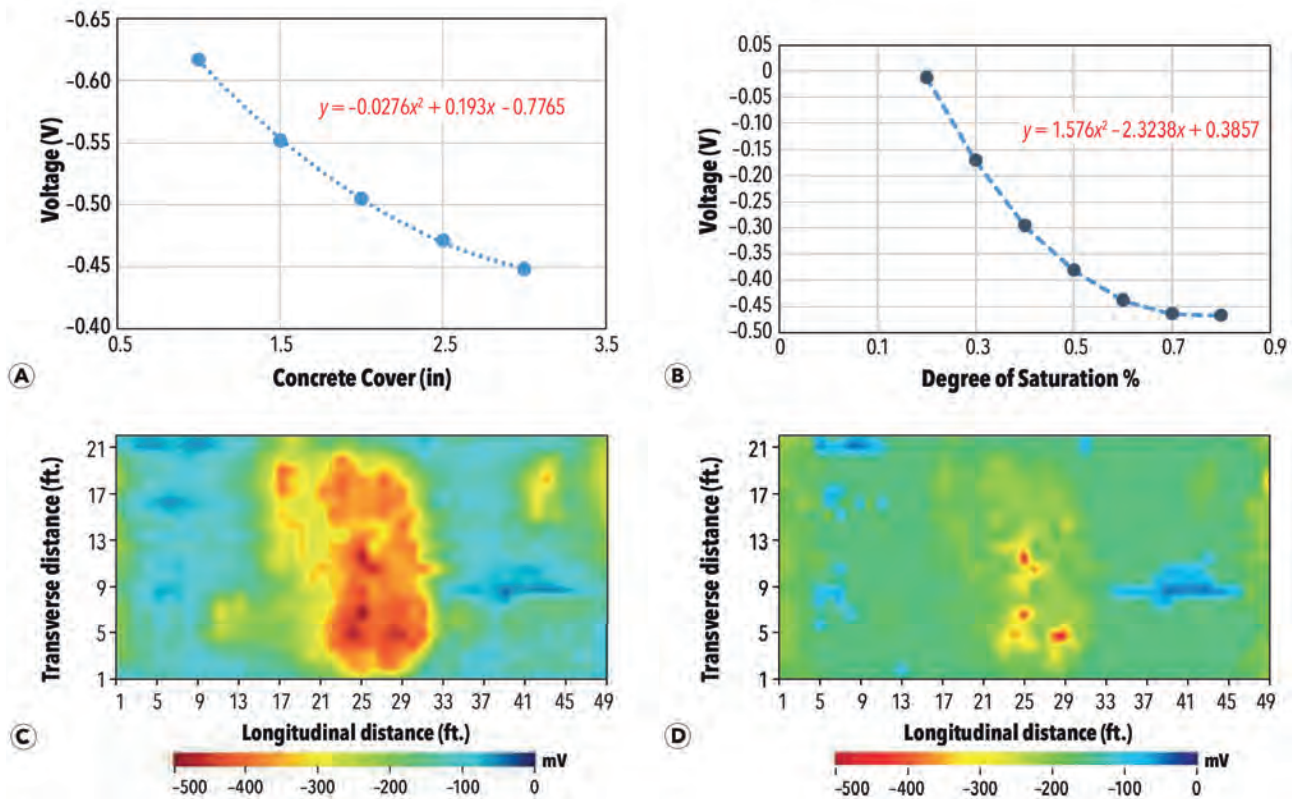


Figure 10. Improved HCP results interpretation: (a) calibration curves for concrete cover and (b) degree of saturation; and condition maps: (c) before and (d) after implementation of the algorithm
 Рис. 10. Покращена інтерпретація результатів HCP: (a) калібрувальні криві для бетонного покриття та (b) ступінь насичення; і карти технічного стану: (c) до і (d) після впровадження алгоритму

has reduced the high potential voltages in the middle of the slab because this area has a thin concrete cover (25 to 38 mm, or 1 to 1.5 in.), as shown in Figure 9b, and also has a higher degree of saturation, as shown in Figure 9a. The reference model that was used to produce the algorithm is the model that has a 40% degree of saturation, a 50 mm concrete cover, and has no delamination as well as no corrosion in the reinforcement steel bar. In general, the algorithm has modified the HCP measurements by shifting the collected values to the right of the scale (fewer negative values), while the right and left edges had almost no changes in the potential values. The changes were primarily controlled by the effect of concrete cover thickness.

Conclusion

NDE will be essential for both the safety of bridges and their economic management. On the safety side, NDE technologies enable the detection and characterization of defects and deterioration on fracture-critical bridge members. On the bridge management side, periodical NDE surveys enable the development of more reliable deterioration, predictive and life-cycle cost models and, thus, timely implementation of preventive maintenance, rehabilitation, and repair. To achieve wide acceptance of NDE in the condition assessment and monitoring of bridges, improvements are needed in the speed of data collection, the ability to deploy NDE technologies on hard-to-reach bridge components, and the NDE data interpretation. The first two will lead to a significant reduction in NDE survey costs, traffic interruptions, and risks for the bridge inspectors and drivers, while the third will lead to an accurate interpretation of the condition. The presented robotic systems are illustrations of the potential for improvements in the speed of data collection, simultaneous deployment of multiple NDE technologies, reduction in the number of bridge inspectors needed to conduct NDE surveys, and accessibility of all bridge components. At the same time, the presented examples of enhanced visualization of NDE data and improved interpretation of NDE results through a joint analysis of results of multiple NDE technologies illustrate the potential for both more reliable and intuitive detection of defects and a more objective description of the condition.

Acknowledgments

Some of the presented work was funded by the Federal Highway Administration’s Long Term Bridge Performance (LTBP) Program and by Vingroup Joint Stock Co. and supported by Vingroup Innovation Foundation (VINIF) under project code VINIF.2020.NCUD.DA094.

References

AASHTO. 2011. AASHTO TP 95-11: Standard Test Method for Surface Resistivity Indication of Concrete’s Ability to Resist Chloride Ion Penetration. Washington: AASHTO.

Almallah, N., and N. Gucunski. 2019. “Automated Detection and Visualization of Defects Using Constant Phase Data from Air-Coupled Impact Echo Testing of Concrete Decks,” *Proceedings of the 98th Annual Transportation Board Meeting, Washington, DC*.

ASCE. 2021. 2021 *Infrastructure Report Card, American Society of Civil Engineers (ASCE)*. infrastructurereportcard.org.

ASTM. 2015. ASTM C876-15: *Standard test method for corrosion potentials of uncoated reinforcing steel in concrete*. West Conshohocken, PA: ASTM International.

Azari, H., D. Yuan, S. Nazarian, and N. Gucunski. 2012. “Sonic Methods to Detect Delamination in Concrete Bridge Decks: Impact of Testing Configuration and Data Analysis Approach,” *Transportation Research Record: Journal of the Transportation Research Board* 2292 (1): 113–24. <https://doi.org/10.3141/2292-14>

Barnes, C.L., and J.F. Trottier. 2000. “Ground-penetrating Radar for Network-level Concrete Deck Repair Management” *Journal of Transportation Engineering* 126 (3): 257–62. [https://doi.org/10.1061/\(ASCE\)0733-947X\(2000\)126:3\(257\)](https://doi.org/10.1061/(ASCE)0733-947X(2000)126:3(257))

Barnes, C., J.F. Trottier, and D. Forgeron. 2008. “Improved Concrete Deck Evaluation Using GPR by Accounting for Signal Depth-Amplitude Effects” *NDT & E International* 41 (6): 427–33. <https://doi.org/10.1016/j.ndteint.2008.03.005>

Bien, J., L. Elfegren, and J. Olofsson (eds.). 2007. *Sustainable Bridges – Assessment for Future Traffic Demands and Longer Lives, TIP3-CT-2003-001653* within the 6th Framework Programme of EU, ISBN 978-7125-161-0, Wroclaw, Poland.

Daniels, D.J. (ed.). 2004. *Ground Penetrating Radar*. 1st ed. London: The Institution of Engineering and Technology.

De La Haza, A., A.A. Samokrutov, and P.A. Samokrutov. 2013. “Assessment of Concrete Structures Using the Mira and Eyecon Ultrasonic Shear Wave Devices and the SAFT-C Image Reconstruction Technique” *Construction & Building Materials* 38:1276–91. <https://doi.org/10.1016/j.conbuildmat.2011.06.002>

Dinh, K., T. Zayed, F. Romero, and A. Tarussov. 2015. “Method for Analyzing Time-series GPR data of Concrete Bridge Decks” *Journal of Bridge Engineering* 20 (6): 04014086. [https://doi.org/10.1061/\(ASCE\)BE.1943-5592.0000679](https://doi.org/10.1061/(ASCE)BE.1943-5592.0000679)

Dinh, K., N. Gucunski, J. Kim, and T.H. Duong. 2016. “Understanding Depth-Amplitude Effects in Assessment of GPR Data from Concrete Bridge Decks” *NDT & E Journal* 83: 48–58. <https://doi.org/10.1016/j.ndteint.2016.06.004>

Dinh, K., N. Gucunski, and T. Zayed. 2019. “Automated Visualization of Concrete Bridge Deck Condition from GPR Data” *NDT & E International* 102: 120–28. <https://doi.org/10.1016/j.ndteint.2018.11.015>

Dinh, K., and N. Gucunski. 2021. “Factors Affecting the Detectability of Concrete Delamination in GPR Images.” *Construction & Building Materials* 274: 121837. <https://doi.org/10.1016/j.conbuildmat.2020.121837>

Elsener, B.C. Andrade, J. Gulikers, R. Polder, and M. Raupach. 2003. “Half-cell Potential Measurements - Potential Mapping on Reinforced Concrete Structures” *Materials and Structures* 36 (Aug): 461–71. <https://doi.org/10.1007/BF02481526>

Gibson, A., and J.S. Popovics. 2005. “Lamb Wave Basis for Impact-Echo Method Analysis” *Journal of Engineering Mechanics* 131 (4) 438–443. [https://doi.org/10.1061/\(ASCE\)0733-9399\(2005\)131:4\(438\)](https://doi.org/10.1061/(ASCE)0733-9399(2005)131:4(438))

Goeller, A., and B. Jungstadt. 2018. “Mikrowellen-Feuchtescans an großen Bauwerken-Anwendungen des Mikrowellenscanners MOIST SCAN 100.” *Fachtagung Bauwerksdiagnose, Feb. 15–16, Berlin (DGZfP Bau-2018)*, NDT. net Issue: 2018-07.

Gowers, K.R., and S.G. Millard. 1999. “Measurement of Concrete Resistivity for Assessment of Corrosion Severity of Steel Using Wenner Technique.” *ACI Materials Journal* 96 (5): 536–42.

Gucunski, N., A. Imani, F. Romero, S. Nazarian, H Azari, H. Wiggenhauser, P. Shokouhi, A. Taffe, and D. Kutrubes. 2013. *Nondestructive Testing to Identify Concrete Bridge Deck Deterioration, SHRP 2 Report S2-R06A-RR-1*, Transportation Research Board, Washington, D.C.

Gucunski, N., B. Pailles, J. Kim, H. Azari, and K. Dinh. 2016. “Capture and Quantification of Deterioration Progression in Concrete Bridge Decks Through Periodical NDE Surveys.” *Journal*

- of *Infrastructure Systems*, 23 (1). [https://doi.org/10.1061/\(ASCE\)IS.1943-555X.0000321](https://doi.org/10.1061/(ASCE)IS.1943-555X.0000321)
- Gucunski, N., B. Basily, J. Kim, J. Yi, T. Duong, K. Dinh, S.-H. Kee, and A. Maher. 2017. "RABIT: Implementation, Performance Validation and Integration with Other Robotic Platforms for Improved Management of Bridge Decks." *International Journal of Intelligent Robotics and Applications* 1: 271–86. <https://doi.org/10.1007/s41315-017-0027-5>.
- Hornbostel, K., C.K. Larsen, and M.R. Geiker. 2013. "Relationship between Concrete Resistivity and Corrosion Rate – A Literature Review." *Cement and Concrete Composites* 39: 60–72. <https://doi.org/10.1016/j.cemconcomp.2013.03.019>
- Kee, S.H., and N. Gucunski. 2016. "Interpretation of Flexural Vibration Modes from Impact-Echo Testing." *Journal of Infrastructure Systems* 22 (3): 04016009. [https://doi.org/10.1061/\(ASCE\)IS.1943-555X.0000291](https://doi.org/10.1061/(ASCE)IS.1943-555X.0000291)
- Kim, J., N. Gucunski, T.H. Duong, and K. Dinh. 2017. "Three-dimensional Visualization and Presentation of Bridge Deck Condition Based on Multiple NDE Data." *Journal of Infrastructure Systems* 23 (3): B4016012. [https://doi.org/10.1061/\(ASCE\)IS.1943-555X.0000341](https://doi.org/10.1061/(ASCE)IS.1943-555X.0000341)
- Kim, J., N. Gucunski, and K. Dinh. 2019. "Deterioration and Predictive Condition Modeling of Concrete Bridge Decks Based on Data from Periodic NDE Surveys." *Journal of Infrastructure Systems* 25 (2). [https://doi.org/10.1061/\(ASCE\)IS.1943-555X.0000483](https://doi.org/10.1061/(ASCE)IS.1943-555X.0000483)
- Maser, K.R., and W.M. Kim Roddis. 1990. "Principles of Thermography and Radar for Bridge Deck Assessment." *Journal of Transportation Engineering* 116 (5): 583–601. [https://doi.org/10.1061/\(ASCE\)0733-947X\(1990\)116:5\(583\)](https://doi.org/10.1061/(ASCE)0733-947X(1990)116:5(583)).
- Maser, K. and M. Bernhardt. 2000. "Statewide Bridge Deck Survey using Ground Penetrating Radar." *Structural Materials Technology IV - An NDT Conference, Atlantic City, NJ*.
- Maierhofer, C., A. Brink, M. Roellig, and H. Wiggenshauser. 2001. "Detection of Shallow Voids in Concrete Structures with Impulse Thermography and Radar." *Proceedings of the 9th Structural Faults & Repair Conference, London, United Kingdom*.
- Minor, M., H. Dulimarta, G. Danghi, R. Mukherjee, R. Lal Tummala, and D. Aslam. 2000. "Design, implementation, and evaluation of an under-actuated miniature biped climbing robot." *Proceedings. 2000 IEEE/RSJ International Conference on Intelligent Robots and Systems (IROS 2000)* (Cat. No.00CH37113), pp. 1999–2005 vol. 3. <https://doi.org/10.1109/IROS.2000.895264>
- Nazarian, S., M. Baker, and S. Reddy. 1994. "Nondestructive Testing of Pavements and Backcalculation of Moduli: Second Volume." STP 1198, 473–487. Philadelphia, PA.: ASTM Publication. <https://doi.org/10.1520/STP181655>
- Nguyen, S.T., and H.M. La. 2019. "Roller Chain-Like Robot For Steel Bridge Inspection." *Proceedings of the 9th International Conference on Structural Health Monitoring of Intelligent Infrastructure (SHMI-9), St. Louis, MO*.
- Nguyen, S.T., and H.M. La. 2021. "A Climbing Robot for Steel Bridge Inspection." *Journal of Intelligent & Robotic Systems* 102 (4): 75. <https://doi.org/10.1007/s10846-020-01266-1>
- Nguyen, A., G. Klysz, F. Deby, and J.-P. Balayssac. 2017. "Evaluation of Water Content Gradient using a New Configuration of Linear Array Four- Point Probe for Electrical Resistivity Measurement." *Cement and Concrete Composites* 83: 308–22. <https://doi.org/10.1016/j.cemconcomp.2017.07.020>
- Nguyen, S.T., A.Q. Pham, C. Motley, and H.M. La. 2020. "A Practical Climbing Robot for Steel Bridge Inspection." *2020 IEEE International Conference on Robotics and Automation (ICRA)*, pp. 9322–9328, <https://doi.org/10.1109/ICRA40945.2020.9196892>
- Pashoutani, S., J. Zhu, C. Sim, B. Mazzeo, and S. Guthrie. 2020. Development and Implementation of a Moving Nondestructive Evaluation Platform for Bridge Deck Inspection, Report SPR-P1(17) M075, Nebraska DOT.
- Raupach, M., K. Reichling, H. Wiggenshauser, M. Stoppel, G. Dobmann, and J. Kurz. 2009. "BETOSCAN 0 An Instrumented Mobile Robot System for the Diagnosis of Reinforced Concrete Floors." *Proc. 2nd Intl. Conf. on Concrete Repair, Rehabilitation and Retrofitting II, ICCRRR-2, November 24-26, 2008, Cape Town, South Africa, CRC Press*, 651-655.
- Robles, K. P. V., J.-J. Yee, and S.-H. Kee. 2022. "Electrical Resistivity Measurements for Nondestructive Evaluation of Chloride-Induced Deterioration of Reinforced Concrete-A Review." *Materials (Basel)* 15 (8): 2725. <https://doi.org/10.3390/ma15082725>
- Rupnow, T.D., and P.J. Icenogle. 2012. "Surface Resistivity Measurements Evaluated as Alternative to Rapid Chloride Permeability Test for Quality Assurance and Acceptance." *Transportation Research Record: Journal of the Transportation Research Board* 2290 (1): 30–37. <https://doi.org/10.3141/2290-04>
- Sansalone, M., and N.J. Carino. 1989. "Detecting Delaminations in Concrete Slabs with and without Overlays Using the Impact-Echo Method." *ACIMaterials Journal* 86 (2): 175–84.
- Sun, H. B., J.Y. Zhu, and S.Y. Ham. 2018. "Automated Acoustic Scanning System for Delamination Detection in Concrete Bridge Decks." *Journal of Bridge Engineering* 23 (6): 04018027. [https://doi.org/10.1061/\(ASCE\)BE.1943-5592.0001237](https://doi.org/10.1061/(ASCE)BE.1943-5592.0001237)
- Tarussov, A., M. Vandry, and A. De La Haza. 2013. "Condition Assessment of Concrete Structures using a New Analysis Method: Ground-Penetrating Radar Computer-Assisted Visual Interpretation." *Construction & Building Materials* 38:1246–54. <https://doi.org/10.1016/j.conbuildmat.2012.05.026>
- Tirthankar, B., S. Ryan, T. Fletcher, K. Navinda, D. Ross, W. Brett, B. James, H. Karsten, and E. Alberto. 2018. "Magneto: A Versatile Multi-Limbed Inspection Robot." *Proceedings of the 2018 IEEE/RSJ Intern. Conf. on Intelligent Robots and Systems (IROS), Madrid, Spain*, pp. 1–5.
- Washer, G., R. Fenwick, N. Bolleni, and J. Harper. 2009. "Effects of Environmental Variables on Infrared Imaging of Subsurface Features of Concrete Bridges." *Transportation Research Record* 2108 (1): 107–114. <https://doi.org/10.3141/2108-12>
- Zhu, J., and J.S. Popovics. 2007. "Imaging Concrete Structures Using Air-Coupled Impact Echo." *Journal of Engineering Mechanics* 133 (6): 628–40. [https://doi.org/10.1061/\(ASCE\)0733-9399\(2007\)133:6\(628\)](https://doi.org/10.1061/(ASCE)0733-9399(2007)133:6(628))

Permission to Reprint 08.02.2023:

The American Society for Nondestructive Testing, Inc.

CITATION

Materials Evaluation 81(1): 56-66

<https://doi.org/10.32548/2023.me-04289>

©2022 American Society for Nondestructive Testing

НОВА КНИГА



Welding and Joining of Aerospace Materials

Editor: Mahesh Chaturvedi

eBook ISBN: 9780128191415

Paperback ISBN: 9780128191408

Woodhead Publishing Series in Welding and Other Joining Technologies

Welding and Joining of Aerospace Materials, Second Edition, is an essential reference for engineers and designers in the aerospace, materials, welding and joining industries, as well as companies and other organizations operating in these sectors. This updated edition brings together an international team of experts with updated and new chapters on electron beam welding, friction stir welding, weld-bead cracking, and recent developments in arc welding.